π Complexes

DOI: 10.1002/ange.201206111

Cyclopentadienylruthenium π Complexes of Subphthalocyanines: A "Drop-Pin" Approach To Modifying the Electronic Features of Aromatic Macrocycles**

Esmeralda Caballero, Javier Fernández-Ariza, Vincent M. Lynch, Carlos Romero-Nieto, M. Salomé Rodríguez-Morgade, Jonathan L. Sessler,* Dirk M. Guldi,* and Tomás Torres**

In memory of Christian G. Claessens

Molecules that possess a concave shape are especially attractive for the construction of effective recognition sites and supramolecular architectures.[1] When the concave structure consists of an extended, delocalized π system, some features, such as aromaticity, vary as a function of the curvature of the bowl, as well as the face—i.e., *exo* or *endo*—on which the property is measured.[2] Furthermore, the two chemically distinct surfaces, concave or convex, that result from distortions from planarity can exhibit disparate reactivity patterns upon, for example, reactions with electrophiles, formation of supramolecular complexes, or treatment with reactive metal fragments. This can give rise to a greater diversity of structures, reaction products, and, in some cases, additional topologies compared to what is seen in the case of classical, planar structures.[3,4]

Among the several distinct categories of curved π surfaces, boron(III) subphthalocyanines (SubPcs, Scheme 1)[5] are particularly attractive. SubPcs are contracted phthalocyanine analogues made up of three isoindole moieties. The resulting 14-π-electron aromatic system adopts a nonplanar, cone-shaped conformation. The SubPcs display features consistent with nonplanar aromaticity and are characterized by rather unique spectroscopic and electronic features. In addition, SubPcs with C_3 or C_1 symmetries display intrinsic chirality.[6] Taken in concert, these attributes enhance their potential utility as building blocks for the construction of complex molecules. The electronic and physical properties of SubPcs can be modulated by introducing various substituents at the axial (X in Scheme 1)[7] and/or peripheral positions.[5a] The original SubPc backbone has also been subjected to further structural modifications through the preparation of the corresponding subporphyrazines (SubPzs)[8] and subporphyrins (SubPs, Scheme 1).[9,10]

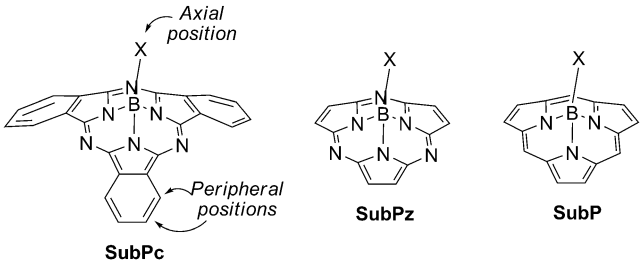

Scheme 1. Chemical structures of SubPc and its SubPz and SubP analogues.

As with other concave systems, the distinct nature of the SubPc faces has been demonstrated. For example, SubPc–C_{60} donor–acceptor hybrids show different electron-transfer abilities related to the different modes of electronic interaction between the two redox units, either through the concave[11] or through the convex[12] faces of the SubPc cone. Surprisingly, however, direct functionalization of the SubPc π faces has not hitherto been reported. This lack of precedent prompted us to explore whether SubPcs and its analogues could behave as π ligands during their reaction with organometallic fragments. Herein we report the synthesis and complete characterization of novel SubPc π complexes in which the arenophilic ruthenium(II) center Cp^*Ru^+ ($Cp^* =$

[*] Dr. E. Caballero, J. Fernández-Ariza, Dr. M. S. Rodríguez-Morgade, Prof. T. Torres
Departamento de Química Orgánica
Universidad Autónoma de Madrid
Cantoblanco, 28049-Madrid (Spain)
E-mail: tomas.torres@uam.es
Prof. V. M. Lynch, Prof. J. L. Sessler
Department of Chemistry and Biochemistry and
Institute for Cellular and Molecular Biology
1 University Station-A5300, University of Texas at Austin
TX 78712-0165 (USA)
E-mail: sessler@mail.utexas.edu
Dr. C. Romero-Nieto, Prof. D. M. Guldi
Department of Chemistry and Pharmacy & Interdisciplinary Center for Molecular Materials (ICMM)
University of Erlangen-Nuremberg
Egerlandstrasse 3, 91058 Erlangen (Germany)
E-mail: dirk.guldi@chemie.uni-erlangen.de
Prof. T. Torres
IMDEA-Nanociencia, c/Faraday, 9, Campus de Cantoblanco
28049- Madrid (Spain)

[**] Support is acknowledged from the U.S. National Science Foundation (grant CHE-1057904 to J.L.S.), the Robert A. Welch Foundation (grant F-1018 to J.L.S.), the Spanish MEC (CTQ2011-24187/BQU and CONSOLIDER INGENIO 2010, CSD2007-00010 on Molecular Nanoscience), the Comunidad de madrid (MADRISOLAR-2, S2009/PPQ/1533), the EU (FP7-ICT-2011.3.6, No: 287818), Fonds der Chemischen Industrie (FCI), and Deutsche Forschungsgemeinschaft (SFB 583).

Supporting information for this article is available on the WWW under http://dx.doi.org/10.1002/anie.201206111.

C_5Me_5) is coordinated to either of the two distinct SubPc π surfaces, namely the concave or convex faces of this classic nonplanar chromophore. As detailed below, this approach involves functionalizing the π surface by dropping an organometallic "pin" at a specific location. To help understand the reactions leading to the formation of the complexes and the effect of π coordination on the electronic features of SubPcs, comparisons with the corresponding axially substituted ruthenoarene SubPzs are also described. Taken in concert, this study provides a complement to established efforts to functionalize porphyrins and related pyrrolic systems with organometallic fragments.[13–15]

We began our investigation with SubPz, since it is a simpler system than SubPc. We envisioned that π complexes of SubPz might be prepared by treating compound **1** (Scheme 2) with a Cp^*Ru^+ salt by a procedure previously reported for the preparation of porphyrin–[14] and porphycene–ruthenocene hybrids.[15] SubPz **1** contains two different aromatic units, namely the pyrrole and the axial benzene ring. Although previous studies on π-indole and isoindole complexes revealed that this metal fragment reacts preferentially with the benzene rings,[16] in the case of porphyrins, π complexes were formed wherein the metals were attached to the pyrrole rings.[14,15,17] It was thus an open question as to whether this particular arenophile (i.e., Cp^*Ru^+) would react with SubPzs and, if so, which of the three available π surfaces (convex, concave, or the aryl moiety present on the axial ligand) would dominate. Treatment of SubPz **1** with excess $[Cp^*Ru(MeCN)_3]PF_6$ in dichloromethane afforded the ruthenoarene π complex **2** exclusively and in 86% yield (Scheme 2).

The structure of **2** was initially assigned by ^{1}H NMR spectroscopy. In particular, as would be expected for a η^6-complex such as **2**, the axial benzene protons are shifted $\delta =$ 1.2–1.6 ppm upfield relative to those of the precursor **1**; presumably, this reflects the diatropic ring current of the cyclopentadienyl anion (see Figure S4 in the Supporting Information). Further confirmation of the structure came from a single-crystal X-ray diffraction analysis (Figure 1). In an effort to force the ruthenium π coordination on the pyrrole rings, the same reaction was attempted starting from SubPz derivatives lacking the axial arene ring, that is, bearing fluorine or chlorine substituents in the axial position. However, only starting materials were recovered in this case.

Subsequently, we examined the formation of SubPc π complexes. Treatment of **3a** with $[Cp^*Ru(MeCN)_3]PF_6$ in dichloromethane yielded a mixture of complexes **4a**, **5a**, and **6a**, in 36%, 11%, and 18% yields, respectively (Scheme 3 and Table S1 in the Supporting Information).

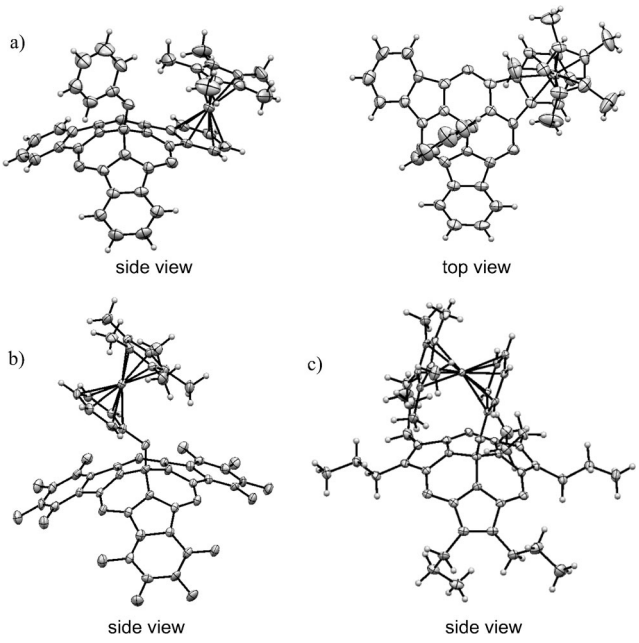

Figure 1. X-ray crystal structures of a) **6a**, b) **4c**, and c) **2** with the thermal ellipsoids drawn at the 50% probability level. Solvent molecules and counteranions are omitted for clarity.

As expected, no ruthenoarene complexed to a pyrrole subunit.[16] However, coordination to both the axial and isoindolic benzene rings was seen. The slightly higher reactivity of the axial benzene ring related to that of the isoindolic benzene ring could arise from the electron-withdrawing substitution pattern in the latter case, which renders the ring more electron poor. In the case of substitution of the isoindole fragment, no dominant reactivity pattern was observed, although a slight (5:3) preference towards *exo* rather than *endo* binding was observed.

As was the case for complex **2**, compound **4a** could easily be distinguished from **5a** and **6a** by ^{1}H NMR spectroscopy. Again, upfield shifts of the protons corresponding to the η^6-coordinated benzene ring were seen (see Figures S9, S13, and S15 in the Supporting Information). The structures of the *endo* (**5a**) and *exo* (**6a**) coordinated compounds were then assigned on the basis of a NOESY NMR study, which revealed a correlation between the methyl groups corresponding to the Cp* subunit and the axial phenoxy group. Such an interaction is only possible in the case of complex **6a** (see Figure S14a,b in the Supporting Information). A single-crystal X-ray diffraction analysis of **6a** (Figure 1) confirmed the structural assignments drawn from the NMR analysis.

Next, we examined whether it was possible to increase the selectivity with which the incoming ruthenium arenophile attacks the π framework of either the axial phenyl or isoindolic benzene

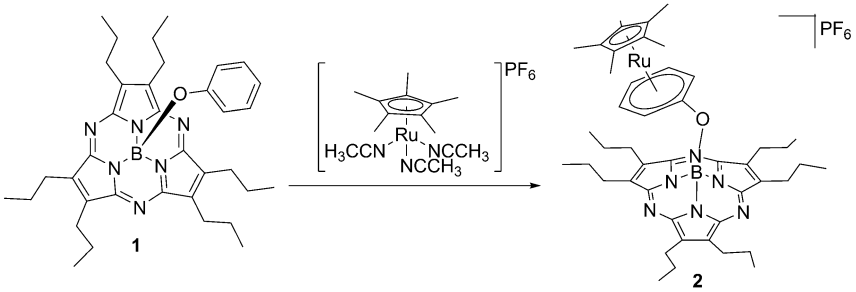

Scheme 2. SubPz π complexes.

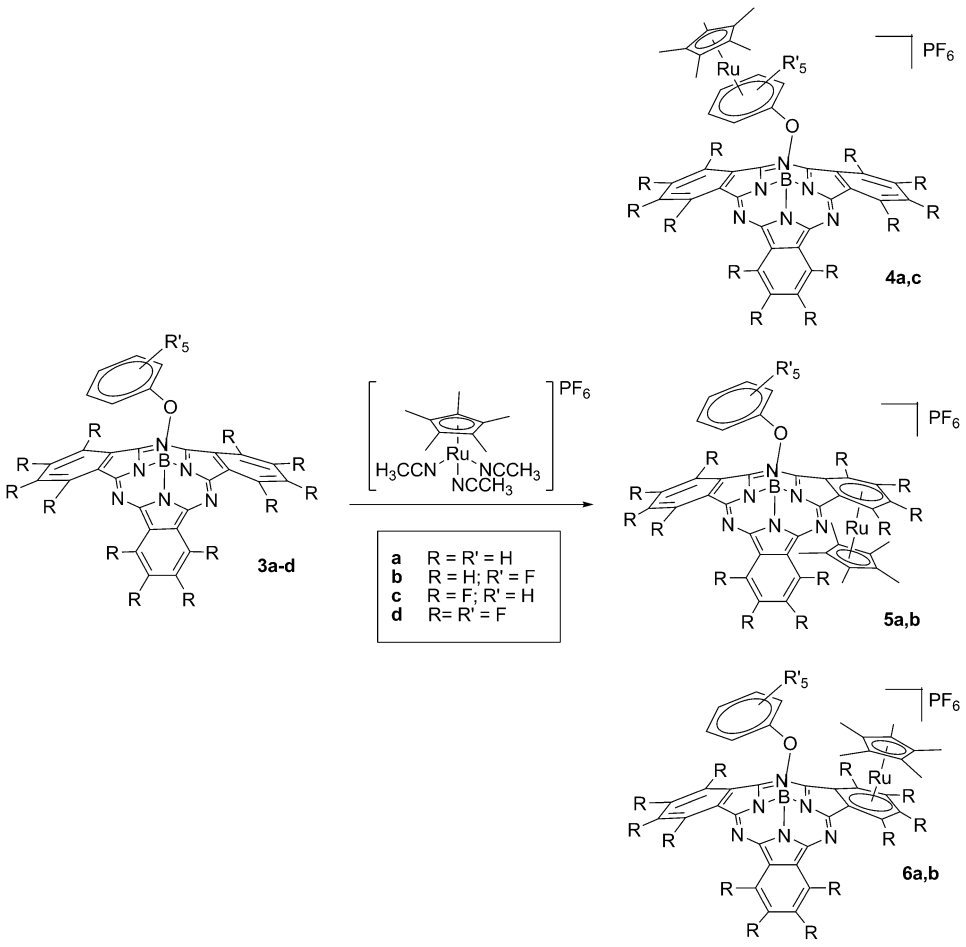

Scheme 3. Synthesis of SubPc π complexes.

ring. With this goal in mind, we elected to elaborate these disparate subunits with fluorine atoms. Here, our thinking was that the presence of such classic electron-withdrawing substituents would serve to reduce the relative reactivity of the subunit in question towards π complexation. In fact, this strategy proved effective. For example, by using SubPc **3b** bearing five fluorine atoms on the axial benzene ring as the precursor, it proved possible to obtain selectively the π complexes **5b** and **6b** of the isoindolic benzene ring in 22% and 52% yield, respectively. In contrast, when dodecafluorinated SubPc **3c** was used as the starting material, the axial substituted complex **4c** was isolated as the exclusive product. In the case where both phenyl rings were perfluorinated, the starting material (SubPc **3d**) was recovered unchanged after being subjected to our standard reaction conditions. The reaction could also be directed to the isoindolic benzene rings by using a SubPc that lacks a phenyl ring. For example, treatment of the fluoroSubPc **7** (in which fluoride serves as the axial substituent) with $[Cp^*Ru(MeCN)_3]PF_6$ in dichloromethane afforded a 2:7 mixture of *endo*- and *exo*-ruthenated compounds **8** and **9** (see Scheme S1 in the Supporting Information). For comparative purposes we also used this organometallic fragment to prepare the η^6-complex of benzene (**10**, see Figures S1–S3 in the Supporting Information).

Inspection of the chemical shifts of the cyclopentadienyl methyl protons for all the compounds reported herein (see Table S1 in the Supporting Information) shows that the values are strongly dependent on how the metallocene is attached to the macrocycle. The largest diatropic effect on the Cp* ligand was observed in the case of the *endo*-coordinated compounds **5a**,**b** and **8**; here, the signals for the cyclopentadienyl methyl protons are shifted upfield by approximately $\delta = 1.7$ ppm with respect to the those of the starting cyclopentadienylruthenium salt. This shift is noticeably larger than that seen with the corresponding phthalocyanine (ca. $\delta =$ 0.7 ppm shift),[16a] porphyrin (ca. 1-1.5 ppm shift),[14] or porphycene (ca. $\delta = 1.1$ ppm shift)[15] complexes. This occurs despite the larger electronic circuits present in these latter porphyrinoids (18 π electrons versus 14 π electrons in the case of the SubPcs). It is also much larger than the exceptionally modest shifts (< 0.1 ppm) seen in the case of the *exo*-bound complexes **6a**,**b** and **9**. An intermediate diatropic shift effect was observed in the case of the axially bound ruthenoarenes **2** and **4a**,**c**; here, the Cp* methyl signals were shifted by about $\delta = 0.5$ ppm with respect to the precursor. On the basis of comparison studies involving the π complex of benzene **10**, for which the Cp* methyl protons are not shifted compared to the starting complex, we ascribe the bulk of the diatropic shielding effect seen in the case of complexes **2** and **4a**,**c** to the subazaporphyrin rather than to the phenyl-containing axial ligand (see Table S1 in the Supporting Information).

We currently rationalize the above spectroscopic differences in structural terms. For example, a single-crystal X-ray diffraction analysis of the *exo*-bound π complex **6a** (Figure 1a) revealed that the Cp* methyl protons reside outside the 14-π-electron aromatic perimeter because of the convex curvature of the SubPc. They are thus expected to be exposed to very different ring-current effects compared to the Cp* methyl protons of the congeners, where π complexation occurs to the axial phenyl moiety or to the SubPc concave face.

Although we have not succeeded in obtaining diffraction grade crystals for the *endo*-bound compounds **5a**,**b**, it is expected that the concave curvature will serve to orient the Cp* methyl protons under the SubPc moiety, where they

should be subjected to a strong aromatic ring current effect. In the case of axial π complexation, a single-crystal X-ray structure of complex **4c** (Figure 1b) reveals an orientation for the Cp* methyl protons that is substantially offset from the SubPc surface. Nevertheless, these protons do fall within the macrocycle perimeter, as would be expected given the chemical shifts observed in the ^{1}H NMR spectra discussed above. In the case of the ostensibly analogous SubPz complex **2** (Figure 1c), the Cp* methyl groups are also displaced from the SubPc surface, although to a much smaller extent than in the case of complex **4c**. In the solid state, all three complexes (**6a**, **4c**, and **2**) for which structural data are available, are characterized by similar bowl-shaped structures. However, the actual degree of curvature depends on the position of the ruthenoarene moiety and the specific choice of macrocycle (SubPc or SubPz). In the case of the SubPc complexes, the bowl depth, as defined by the distance from the lowest edge of the macrocycle (the mean plane of the peripheral six carbon atoms of the benzene rings) to the boron atom, increases from 2.501 Å in the precursor (**3c**)[18] to 2.684 Å in the *exo* complex **6a** and to 2.780 Å in the axial ruthenoarene **4c**.

The effect of π coordination was also analyzed by UV/Vis spectroscopy. In the case of the SubPz complex **2**, the effect of metal coordination on the absorption spectrum proved minimal (see Figure S7 in the Supporting Information). Likewise, π coordination to the axial phenoxy group in the case of the SubPcs (i.e., forming complexes **4a**,**c**) gave rise to only modest changes, namely a 5 nm bathochromic shift of the Q-like band (Figure 2a and Figure S33 in the Supporting Information). On the other hand, and in accord with what might be expected, coordination of the ruthenium center to the isoindolic benzene rings produced more substantial perturbations. In this case, the complexes displayed similarly sharp Q bands and an additional weak feature between 397 and 411 nm, which is assigned to a charge-transfer (CT) transition. Relative to the relevant precursor (**3a** and **3b**), *exo* π coordination gives rise to a 14 nm bathochromic shift of the Q band (complexes **6a** and **6b**; Figure 2a,b). However, an even greater spectral perturbation was seen when π coordination takes place on the concave face of the SubPc; in this case, a red shift of 24 nm is seen for **5b** relative to its precursor, **3b** (Figure 2b).

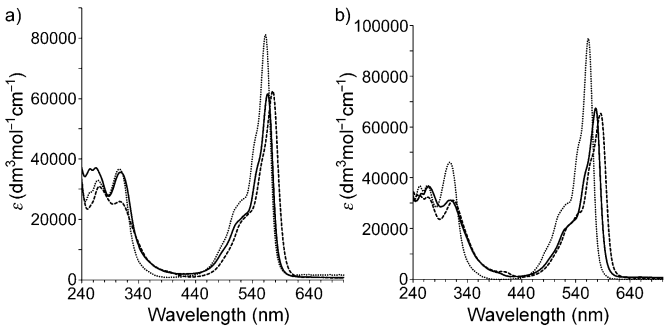

Figure 2. Electronic spectra of a) precursor **3a** (dotted line) its π complexes **4a** (solid line) and **6a** (dashed line) in $CHCl_3$, and b) precursor **3b** (dotted line), its *endo* and *exo* π complexes **5b** (dashed line) and **6b** (solid line) in $CHCl_3$.

The electrochemical properties of the isolated π complexes were examined and compared with those of their precursors by cyclic voltammetry (see Figure S41, S42, S43, and S44 in the Supporting Information) and differential pulse voltammetry (DPV) of solutions in CH_2Cl_2 containing 0.10 M Bu_4NPF_6 as the supporting electrolyte (Table 1 and Table S2 in the Supporting Information give the redox potentials and the HOMO–LUMO gaps derived from these measurements). While $[Cp^*Ru(MeCN)_3]PF_6$ displays only a reversible oxidation process at 0.32 V (see Table S2 in the Supporting Information), reference compound **10** was found to resist oxidation and reduction within the potential window of dichloromethane. On the other hand, SubPz **2** exhibits two reversible redox processes that we, therefore, assigned to the macrocycle. The attachment of the Cp*Ru moiety to the axial position of SubPz **1** shifts the first reduction peak in the anodic direction by 200 mV, from −1.72 to −1.52 V. The first oxidation peak is also shifted by 140 mV in the same direction, from +0.83 to +0.97 V. In other words, the SubPz π complex **2** is considerably easier to reduce and more difficult to oxidize than its precursor **1**. It is interesting to note that, as a general rule, the axial electron-withdrawing groups, such as fluorine, have only a small effect on the redox properties of SubPzs. For example, replacing the phenoxy group in **1** by a boron-coordinated fluoride anion (**11**, see Figure S41 in the Supporting Information) has little effect on the reduction potential and shifts the oxidation potential in the anodic direction by only 10 mV (see Table 1).

Table 1: Electrochemical oxidation and reduction data for the SubPzs and SubPcs studied.[a]

	E_p^{1},red	E_p^{2},red	E_p^{3},red	E_p^{4},red	E_p^{1},ox	E_p^{2},ox
1	−1.72	–	–	–	+0.83	–
2	−1.52	–	–	–	+0.97	–
11	−1.72	–	–	–	+0.84	–
3a	−1.54	−2.05	−2.39	−2.50	+0.57	–
4a	−1.37	−1.94	−2.11	−2.38	+0.72	+1.16
6a	−1.30	−1.79	−2.17[b]	–	+0.77	+1.22[b]
3b	−1.47	−2.03	−2.31	−2.44	+0.64	+1.35
5b	−1.16	−1.69	−2.27	−2.53	+0.92	+1.13
6b	−1.23	−1.75	−2.17	−2.45	+0.82	–
3c	−1.04	−1.65	−2.29	–	+1.00	–
4c	−0.88	−1.54	−1.95	−2.17	+1.00	–
7	−1.52	−2.00	−2.40	–	+0.55	–
8+**9**	−1.25	−1.76	−2.23	–	+0.74	–

[a] Measurements were made in CH_2Cl_2 containing Bu_4NPF_6 as the supporting electrolyte. E_p values (from DPV at RT) are in V versus the ferrocenium/ferrocene couple (Fc^+/Fc). [b] In the window limit.

SubPcs are easier to reduce and oxidize electrochemically than SubPzs. The SubPc precursors **3a–c** showed four reversible reduction peaks, as well as one or two oxidation processes. Substitution with 12 fluorine atoms at the periphery of the macrocycle shifts all the redox processes to more positive values.[19] In particular, the first reduction peak of **3a** is shifted in the anodic direction from −1.54 V to −1.04 V (500 mV shift) in **3c**, while the first oxidation peak moves

from +0.57 V to +1.00 V (430 mV shift). As is the case for the SubPz discussed above, the effect of changes to the axial ligand is more modest. For example, the synthetic attachment of five fluorine atoms to the axial phenoxy ring shifts the potentials towards positive potentials, albeit only by 70 mV (for both reduction and oxidation).

The introduction of a ruthenoarene fragment at any position on the SubPcs also produces readily apparent anodic shifts. The extent of these shifts increases for these π complexes in the following order: axial position < *exo* coordinated < *endo* coordinated. Thus, for example, the first reduction process appears at −1.37 V for **4a** (170 mV shift relative to **3a**)[20] and −0.88 V for **4c** (160 mV shift relative to **3c**). Likewise, the precursor **3b** exhibits a first reduction peak at −1.47 V, while the same redox process occurs at −1.23 V in the case of the *exo*-coordinated SubPc **6b** (240 mV shift). A 290 mV shift is also seen in the case of the *endo* isomer **5b** relative to the same starting material. A similar pattern was seen for the oxidation processes, with the exception of the dodecafluorinated compounds **3c** and **4c**. Here, the oxidation peak remains invariant on going from the precursor to the π complex.

The HOMO–LUMO gaps were calculated using the electrochemical data (Table S2 in the Supporting Information). The estimated values generally reflect what would be inferred from the observed optical spectra. The one exception is compound **4c**, for which a value considerably lower than that of the precursor **3c** is calculated. This could reflect a combination of steric and electronic effects associated with the fluorine substituents that are not readily accounted for by the modeling program.

SubPcs and SubPzs are known to interact well with excited-state quenchers, such as electron donors, electron acceptors, energy acceptors, and agents that facilitate intersystem crossing. In light of this, we probed the excited-state features of **4c**, **5b**, and **6b** and compared them with the respective precursors **3c** and **3b**. In line with what was observed by UV/Vis spectroscopy, only a slight effect is seen on the SubPc and SubPz singlet excited state when the ruthenoarene fragment is in the axial position. We determined fluorescence maxima at 578 and 583 nm, fluorescence quantum yields of 0.27 and 0.25, and fluorescence lifetimes of 1.7 and 1.5 ns, for **3c** and **4c**, respectively. Likewise, we observed in pump probe experiments (Figures S45 and S46 in the Supporting Information) that the SubPc singlet excited states of **3c** and **4c**—maxima at 430, 600, 615, 750, 800, 910, and 1100 nm and minima at 550, 574, and 630 nm—transform with the same (1.5 ± 0.2) ns kinetics into the corresponding SubPc triplet excited states—maxima at 460, 610, and 790 nm and minima at 550 and 570 nm.[21] In stark contrast, *endo* and *exo* positioning of the ruthenocene fragment changes the SubPc singlet excited-state features rather dramatically. In particular, the steady-state and time-resolved attributes of **5b** and **6b** differ significantly from those noted for **3b**. In terms of steady-state measurements, the fluorescence quantum yields are 0.26, 2.9×10^{-4}, and 1.2×10^{-3}, while the corresponding fluorescence maxima are 572, 583, and 593 nm for **3b**, **5b**, and **6b**, respectively.

Detailed time-resolved analyses (see Figures S47–S49 in the Supporting Information) were also carried out to investigate the above findings. These investigations revealed that **3b**, **5b**, and **6b** give rise to singlet excited-state decays of (1600 ± 100), (3.3 ± 0.2), and (4.2 ± 0.1) ps, respectively. It is, however, the SubPc triplet excited states—maxima at 460, 610, and 790 nm and minima at 555 and 575 nm—that evolve from a more effective intersystem crossing in **5b** and **6b** compared to **3b**. Support for this hypothesis came from phosphorescence measurements of singlet oxygen; these revealed quantum yields for **5b** and **6b** as high as 0.46 and 0.39, respectively, which contrast the much lower values of 0.25 found for **3b**. Interestingly, the overall deactivation of the excited state follows the trend noted in the electrochemically induced anodic shifts, namely axial substitution (**4c**) < *exo* coordinated (**6b**) < *endo* coordinated (**5b**).

In summary, cyclopentadienylruthenium π complexes of subporphyrazines and subphthalocyanines have been prepared for the first time. The resulting complexes highlight a new approach to the functionalization of subazaporphyrins. The curved SubPc surface shows higher reactivity towards metal π coordination on its convex side than on the concave one. However, ruthenoarenes fused on the SubPc concave face give rise to a stronger perturbation of the electronic and spectral features of the macrocycle. In turn, the concave side shows a more effective diatropic effect on the methyl signals of the bound cyclopentadienyl ligand. Fusion of the cyclopentadienylruthenium unit to any of the reactive axial, *endo* or *exo* π surfaces produces subazaporphyrins that are easier to reduce and more difficult to oxidize than the parent complexes. The effect of π-metallocene complexation is considerably larger than that produced by exhaustive fluorination of an axially coordinated, or one or more isoindolic benzene rings. It also has the advantage of allowing "drop-pin" functionalization, wherein a specific π surface may be modified in a way that is not currently possible using other known approaches.

Received: July 30, 2012
Published online: October 9, 2012

Keywords: arene ligands · π complexes · ruthenium · subphthalocyanines · subporphyrazines

[1] A. Szumna, *Chem. Soc. Rev.* **2010**, *39*, 4274–4285.
[2] a) M. Mascal, *J. Org. Chem.* **2007**, *72*, 4323–4327; b) E. Kleinpeter, S. Klod, A. Koch, *J. Org. Chem.* **2008**, *73*, 1498–1507.
[3] a) S. N. Spisak, A. V. Zabula, A. S. Filatov, A. Y. Rogachev, M. A. Petrukhina, *Angew. Chem. Int. Ed.* **2011**, *50*, 8090–8094; b) S. Fedi, F. Laschi, P. Zanello, *Inorg. Chem.* **2007**, *46*, 10901–10906; c) A. S. Filatov, M. A. Petrukhina, *Coord. Chem. Rev.* **2010**, *254*, 2234–2246, and references therein.
[4] a) D. Vijay, H. Sakurai, V. Subramanian, G. N. Sastry, *Phys. Chem. Chem. Phys.* **2012**, *14*, 3057–3065, and references therein; b) P. Zanello, S. Fedi, F. Fabrizi de Biani, G. Giorgi, T. Amaya, H. Sakane, T. Hirao, *Dalton Trans.* **2009**, 9192–9197; c) M. Okumura, Y. Nakanishi, K. Kinoshita, S. Yamada, Y. Kitagawa, T. Kawakami, S. Yamanaka, T. Amaya, T. Hirao, *Int. J. Quantum Chem.* **2012**, DOI: 10.1002/qua.24057.

[5] a) C. G. Claessens, D. González-Rodríguez, T. Torres, *Chem. Rev.* **2002**, *102*, 835 – 853; b) N. Kobayashi, *Synthesis and Spectroscopic Properties of Phthalocyanine Analogs*, in *The Porphyrin Handbook*, *Vol. 15* (Eds.: K. M. Kadish, K. M. Smith, R. Guillard), Academic Press, San Diego, **2003**, pp. 161 – 262; c) T. Torres, *Angew. Chem. Int. Ed.* **2006**, *45*, 2834 – 3837.

[6] a) C. G. Claessens, T. Torres, *Tetrahedron Lett.* **2000**, *41*, 6361 – 6365; b) N. Kobayashi, *Coord. Chem. Rev.* **2001**, *219 – 221*, 99 – 103; c) S. Shimizu, A. Miura, S. Khene, T. Nyokong, N. Kobayashi, *J. Am. Chem. Soc.* **2011**, *133*, 17322 – 17328.

[7] a) A. K. Eckert, M. S. Rodríguez-Morgade, T. Torres, *Chem. Commun.* **2007**, 4104 – 4106; b) M. S. Rodríguez-Morgade, C. G. Claessens, A. Medina, D. González-Rodríguez, E. Gutierrez-Puebla, A. Monge, I. Alkorta, J. Elguero, T. Torres, *Chem. Eur. J.* **2008**, *14*, 1342 – 1350; c) J. Guilleme, D. González-Rodríguez, T. Torres, *Angew. Chem. Int. Ed.* **2011**, *50*, 3506 – 3509.

[8] a) M. S. Rodríguez-Morgade, S. Esperanza, T. Torres, J. Barberá, *Chem. Eur. J.* **2005**, *11*, 354; b) J. R. Stork, J. J. Brewer, T. Fukuda, J. P. Fitzgerald, G. T. Yee, A. Y. Nazarenko, N. Kobayashi, W. S. Durfee, *Inorg. Chem.* **2006**, *45*, 6148 – 6151; c) G. M. Aminur Rahman, D. Lüders, M. S. Rodríguez-Morgade, E. Caballero, T. Torres, D. M. Guldi, *ChemSusChem* **2009**, *2*, 330 – 335.

[9] a) Y. Inokuma, J. H. Kwon, T. K. Ahn, M. C. Yoo, D. Kim, A. Osuka, *Angew. Chem. Int. Ed.* **2006**, *45*, 961 – 964; b) E. A. Makarova, S. Shimizu, A. Matsuda, E. A. Luk'yanets, N. Kobayashi, *Chem. Commun.* **2008**, 2109 – 2111; c) N. Kobayashi, Y. Takeuchi, A. Matsuda, *Angew. Chem. Int. Ed.* **2007**, *46*, 758 – 760; d) Y. Takeuchi, A. Matsuda, N. Kobayashi, *J. Am. Chem. Soc.* **2007**, *129*, 8271 – 8281; e) Y. Inokuma, Z. S. Yoon, D. Kim, A. Osuka, *J. Am. Chem. Soc.* **2007**, *129*, 4747 – 4761.

[10] For recent reviews, see a) Y. Inokuma, A. Osuka, *Dalton Trans.* **2008**, 2517 – 2526; b) A. Osuka, E. Tsurumaki, T. Tanaka, *Bull. Chem. Soc. Jpn.* **2011**, *84*, 679 – 697.

[11] a) D. González-Rodríguez, E. Carbonell, G. de Miguel Rojas, C. Atienza Castellanos, D. M. Guldi, T. Torres, *J. Am. Chem. Soc.* **2010**, *132*, 16488 – 16500; b) D. González-Rodríguez, E. Carbonell, D. M. Guldi, T. Torres, *Angew. Chem. Int. Ed.* **2009**, *48*, 8032 – 8036.

[12] a) R. S. Iglesias, C. G. Claessens, T. Torres, G. M. Aminur Rahman, D. M. Guldi, *Chem. Commun.* **2005**, 2113 – 2115; b) D. González-Rodríguez, T. Torres, M. A. Herranz, L. Echegoyen, E. Carbonell, D. M. Guldi, *Chem. Eur. J.* **2008**, *14*, 7670 – 7679; c) D. González-Rodríguez, T. Torres, D. M. Guldi, J. Rivera, M. A. Herranz, L. Echegoyen, *J. Am. Chem. Soc.* **2004**, *126*, 6301 – 6313.

[13] L. Cuesta, J. L. Sessler, *Chem. Soc. Rev.* **2009**, *38*, 2716 – 2729.

[14] L. Cuesta, E. Karnas, V. M. Lynch, J. L. Sessler, W. Kajonkijya, W. Zhu, M. Zhang, Z. Ou, K. M. Kadish, K. Ohkubo, S. Fukuzumi, *Chem. Eur. J.* **2008**, *14*, 10206 – 10210.

[15] L. Cuesta, E. Karnas, V. M. Lynch, P. Chen, J. Shen, K. M. Kadish, K. Ohkubo, S. Fukuzumi, J. L. Sessler, *J. Am. Chem. Soc.* **2009**, *131*, 13538 – 13547.

[16] a) S. M. Contakes, S. T. Beatty, K. K. Dailey, T. B. Rauchfuss, D. Fenske, *Organometallics* **2000**, *19*, 4767 – 4774; b) S. Chen, V. Carperos, B. Noll, R. J. Swope, M. Rakowski DuBois, *Organometallics* **1995**, *14*, 1221 – 1231.

[17] a) K. K. Dailey, T. B. Rauchfuss, *Angew. Chem. Intl. Ed. Engl.* **1996**, *35*, 1833 – 1835; b) K. K. Dailey, T. B. Rauchfuss, *Polyhedron* **1997**, *16*, 3129 – 3136.

[18] J.-Y. Liu, H.-S. Yeung, W. Xu, X. Li, D. K. P. Ng, *Org. Lett.* **2008**, *10*, 5421 – 5424.

[19] a) D. González-Rodríguez, T. Torres, M. M. Olmstead, J. Rivera, M. A. Herranz, L. Echegoyen, C. Atienza Castellanos, D. M. Guldi, *J. Am. Chem. Soc.* **2006**, *128*, 10680 – 10681; b) G. E. Morse, M. G. Helander, J. F. Maka, Z.-H. Lu, T. P. Bender, *ACS Appl. Mater. Interfaces* **2010**, *2*, 1934 – 1944.

[20] The first SubPc oxidation and reduction peaks are comparable to those reported for an axially assembled ferrocenyl subPc dyad: P. V. Solntsev, K. L. Spurgin, J. R. Sabin, A. A. Heikal, V. N. Nemykin, *Inorg. Chem.* **2012**, *51*, 6537 – 6547.

[21] The same trend emerges for a comparison between SubPzs **1** and **2** that feature identical fluorescence, singlet–singlet, and triplet–triplet characteristics.

